



Abbreviated liver magnetic resonance imaging with a second-shot arterial phase image to assess the viability of treated hepatocellular carcinoma after non-radiation locoregional therapy

Il Wan Son¹
 Seung Baek Hong²
 Nam Kyung Lee²
 Suk Kim²
 Hyung Il Seo³
 Young Mok Park³
 Byeong Gwan Noh³
 Jong Hyun Lee⁴

¹Busan Centum Hospital, Clinic of Radiology, Busan, Korea

²Department of Radiology, Biomedical Research Institute, Pusan National University Hospital, Pusan National University School of Medicine, Busan, Korea

³Department of Surgery, Biomedical Research Institute, Pusan National University Hospital, Pusan National University School of Medicine, Busan, Korea

⁴Department of Internal Medicine, Biomedical Research Institute, Pusan National University Hospital, Pusan National University School of Medicine, Busan, Korea

Corresponding author: Seung Baek Hong

E-mail: cinematiclife7@hanmail.net

Received 02 June 2025; revision requested 29 June 2025; accepted 23 July 2025.



Epub: 11.09.2025

Publication date: 02.03.2026

DOI: 10.4274/dir.2025.253482

PURPOSE

To evaluate the feasibility of abbreviated liver magnetic resonance imaging (AMRI) with a second-shot arterial phase (SSAP) image for the viability of treated hepatocellular carcinoma (HCC) after non-radiation locoregional therapy (LRT).

METHODS

We retrospectively enrolled patients with non-radiation LRT for HCC who underwent the modified gadoteric acid-enhanced liver MRI protocol, which includes routine dynamic and SSAP imaging after the first and second injection of gadoteric acid, respectively (6 mL and 4 mL, respectively), and an available reference standard for tumor viability in the treated HCC between March 2021 and February 2022. Two radiologists independently reviewed the full-protocol MRI (FP-MRI) and AMRI with SSAP. For the FP-MRI, observations were assigned using the Liver Imaging Reporting and Data System treatment response (LR-TR) algorithm v.2024. In the AMRI with SSAP, the observations were assigned using the abbreviated LR-TR category according to the arterial mass-like enhancement in SSAP. Ancillary features, such as diffusion restriction and T2-weighted mild-to-moderate hyperintensity, were also optionally used.

RESULTS

Of the 95 patients (70 men and 25 women; mean age, 68.7 years), 42 (44.2%) had viable lesions and 53 (55.8%) had non-viable lesions. The scan time of the simulated AMRI was significantly shorter than the FP-MRI (7.6±0.49 and 23.6±0.50 min, respectively; $p < 0.001$). For evaluating the viability of treated HCC, there were no significant differences in the sensitivity and specificity between the FP-MRI and AMRI with SSAP (sensitivity, 85.7% vs. 80.1%, $P = 0.500$; specificity, 96.2% vs. 96.2%, $P = 1.000$).

CONCLUSION

The abbreviated LR-TR score in AMRI with SSAP showed non-inferior diagnostic performance to FP-MRI in terms of evaluating the viability for the treated HCC, which may be helpful in clinical practice alongside a decreased scan time.

CLINICAL SIGNIFICANCE

Abbreviated liver MRI with SSAP may be helpful for evaluating the viability of treated HCC in practice, while also providing a decreased scan time.

KEYWORDS

Hepatocellular carcinoma, Liver Imaging Reporting and Data System, treatment response, magnetic resonance imaging, gadoteric acid

Hepatocellular carcinoma (HCC) is the fourth leading cause of cancer-related deaths and the sixth most common cancer in the world.¹ Dynamic contrast-enhanced computed tomography (CT) and magnetic resonance imaging (MRI) are imaging modalities broadly used to assess the response of HCC to locoregional therapy (LRT). Because of the significant correlation between treatment response and patient prognosis, the precise and reliable evaluation of treatment response using imaging tests is crucial.²

The Liver Imaging Reporting and Data System (LI-RADS) introduced a treatment response algorithm, wherein, after LRT, the standardized approach can be applied to evaluate the treatment response using contrast-enhanced CT or MRI.³ Unlike the modified response evaluation criteria for solid tumors, per-lesion treatment response is assessed using the LI-RADS treatment response (LR-TR) algorithm. Treated lesions can be categorized into three LR-TR categories, namely viable, non-viable, and equivocal.⁴ In 2024, a revised version of the LR-TR algorithm, divided into categories for post-radiation therapy and non-radiation LRT groups, was released. The LI-RADS non-radiation TR algorithm v.2024 adopts a single major feature, “mass-like enhancement (any degree, any phase)” for assessing viability of treated HCC on CT or MRI. Additionally, for a treated lesion with uncertain mass-like enhancement, two MRI-based ancillary features, such as “diffusion restriction (any degree)” or “mild to moderate T2 hyperintensity”, can optionally be used to upgrade from LR-TR equivocal to LR-TR viable.⁵

Gadoxetic acid (Primovist; Bayer Pharma, Berlin, Germany) is a hepatocyte-specific contrast agent in liver MRI, used to identify and characterize various hepatic lesions because it provides the additional benefit

of delayed hepatobiliary phase (HBP) imaging.⁶⁻⁸ Although gadoxetic acid liver MRI provides the aforementioned advantage, arterial phase (AP) images are more frequently degraded than those of other gadolinium-based contrast agents because of contrast-related transient severe motion (TSM).⁹ To date, various strategies, such as advanced motion-insensitive MRI sequences, modifications to the injection protocol, and multiple APs, have been reported.¹⁰⁻¹⁷ Several studies reported the usefulness of second-shot arterial phase (SSAP) images in gadoxetic acid-enhanced liver MRI.¹⁷⁻¹⁹ Park et al.¹⁷ reported that SSAP images showed significantly fewer motion artifacts compared with the original AP images.

Several studies on SSAP have demonstrated the potential of abbreviated liver MRI (AMRI) with preserved diagnostic performance, compared with full-protocol MRI (FP-MRI). For evaluating hepatic metastasis, AMRI had a significantly shorter acquisition time compared to FP-MRI, while maintaining image quality, diagnostic performance, and visual vascularity.¹⁸ To assess HCC using AMRI with SSAP, the modified LI-RADS category incorporating HBP hypointensity as a major feature demonstrated a high concordance rate (97.4%) with the standard LI-RADS category. In addition, the recall rate was reduced not only in the surveillance but also diagnosis of HCC with AMRI using the SSAP protocol.¹⁹

Although several studies have investigated SSAP,¹⁷⁻¹⁹ further validation is required to establish the usefulness of the SSAP protocol in evaluating the viability of HCC after LRT. Therefore, we investigated the efficacy

of AMRI with SSAP in determining the LR-TR category in patients with HCC following non-radiation LRT.

Methods

This retrospective study was approved by the Ethics Committee: Institutional Review Board of Pusan National University Hospital (approval number: 22504-018-150; approval date: May 9, 2025). Due to the retrospective nature of the study, the requirement for informed consent was waived.

Patients

At our institution, liver MRI was performed between March 2021 and February 2022 using a modified injection protocol that included routine dynamic and SSAP imaging after the first (6 mL) and second (4 mL) injections, respectively. The excellence of the modified injection protocol has been reported in previous studies.¹⁷⁻¹⁹

We used our institute’s electronic database to identify eligible patients. The inclusion criteria were as follows: 1) patients with non-radiation LRT for HCC who underwent the modified liver MRI protocol, and 2) an available reference standard for tumor viability in the treated observation. Before LRT, the diagnosis of HCC was made using the reference standard defined by LI-RADS v.2018³ or pathologic results. The exclusion criteria included: 1) misregistration of subtraction images and 2) diffuse infiltrative HCC. For patients with multiple lesions, the largest targeted lesion per patient was selected for analysis. A flow diagram of our study is provided in Figure 1.

Main points

- The abbreviated Liver Imaging Reporting and Data System treatment response score in abbreviated liver magnetic resonance imaging (AMRI) with second-shot arterial phase (SSAP) showed non-inferior diagnostic performance compared with full-protocol MRI (FP-MRI) in evaluating the viability for the treatment of hepatocellular carcinoma.
- The scan time of the AMRI can be significantly shorter compared with FP-MRI.
- The mean motion score of the original AP was significantly higher than that of the three SSAPs.

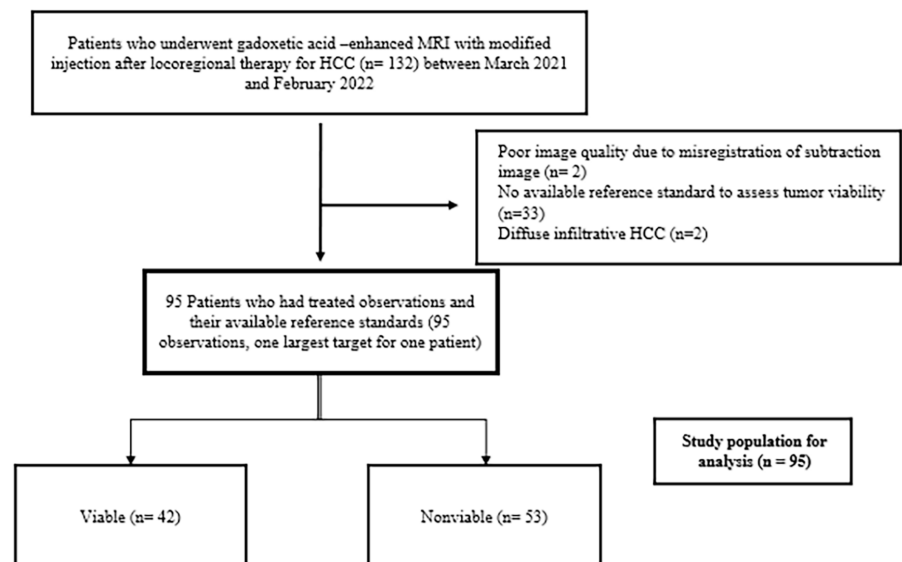


Figure 1. Flow diagram of the study. HCC, hepatocellular carcinoma.

Reference standard

Reference standards for viable tumors in the treated observations were as follows: 1) pathological confirmation (interval between MRI and operation <4 weeks) or 2) tumor staining in transcatheter arterial chemoembolization. Digital subtraction angiography (DSA) images were reviewed to evaluate the tumor staining. Non-viable tumors were considered based on the following: 1) pathological confirmation (total necrosis) or 2) stability or a decrease in the size of the targeted lesion on follow-up images (at least a 6-month interval from MRI) with no evidence of treatment.

Magnetic resonance imaging techniques

All eligible patients had MRI examinations using a 3.0 T MR scanner (Magnetom Skyra; Siemens Healthineers, Erlangen, Germany) with a 32-element spine matrix coil and a 30-element body matrix coil. Non-contrast-enhanced sequences, such as T1-weighted dual-gradient echo in/out-of-phase sequences, T2-weighted breath-hold half-Fourier acquisition single shot turbo spin echo images, T2-weighted respiratory-triggered single shot images, and diffusion-weighted echo planar images with three b-values (0, 500, and 1,000 s/mm²). For liver MRI, all patients received 10 mL of gadoxetic acid (Primovist; Bayer Schering Pharma) at a rate of 1 mL/s. Routine AP images (15–20 seconds after gadoxetic acid injection), portal venous (60–90 seconds after gadoxetic acid injection), transitional (180 seconds after gadoxetic acid injection), and HBP (20 minutes after gadoxetic acid injection) images were acquired. After the end of the routine MRI, 4 mL of gadoxetic acid was administered. SSAP images were subsequently acquired in the same manner (Figure 2).

Routine AP and SSAP images were acquired in one and three-phased, respectively.

Subtracted images were acquired from the SSAP images. Details of the MRI sequence parameters are provided in Table 1.

Image analysis

One of the radiologists with 22 years of experience in abdominal radiology collected the MRI images and information on the size and location of the target lesions before the review process.

Two radiologists, with 13 and 11 years of experience in liver MRI, respectively, independently and randomly reviewed the FP-MRI and simulated AMRI sets, while being unaware of the clinical data and reference standard. During the review, the reviewers analysed two separate MRI sessions with a 4-week interval to reduce recall bias.

First review session

For FP-MRI, both reviewers classified observations based on the LR-TR algorithms (LR-TR viable, LR-TR equivocal, or LR-TR non-viable). Considering both routine AP and SSAP, the “viable” category was considered for mass-like enhancement (any degree, any

phase) within or along the targeted lesion. In addition, ancillary features, such as diffusion restriction and T2-weighted mild-to-moderate hyperintensity, were optionally used.⁵

During the first session, the degree of motion artifact in routine AP, and first, second, and third-phase SSAP was recorded using the following scoring scale:⁹ 1) no motion artifact; 2) minimal degree; 3) moderate degree, not significantly affecting diagnosis; 4) severe degree, degraded but interpretable images; and 5) extensive degree, non-diagnostic images.

Second review session

The simulated AMRI set comprised diffusion-weighted images, T2-weighted images, HBP images, and SSAP images (Figure 2). Both reviewers analyzed the arterial hyper-enhancement using the SSAP image and its subtraction image. Accordingly, a modified version of the LR-TR algorithm using the abbreviated LR-TR (abbLR-TR) categories (abbLR-TR viable, abbLR-TR equivocal, or abbLR-TR non-viable) was devised. Both reviewers assigned the abbLR-TR classification according to the mass-like enhancement us-

Table 1. Details of the MRI sequence parameters

	Sequence	
	T1 VIBE (routine)*	T1 VIBE (SSAP)
Repetition time, ms	4.0	4.0
Echo time, ms	1.9	1.9
Flip angle, °	13	13
Field of view	380 x 285	380 x 285
Matrix	384 x 202	320 x 144
Section thickness, mm	3.5	3.5
Acquisition time (sec)	15	15
No. of phases acquired	1	3
Parallel acceleration factor [†]	2 x 2	2 x 2

*Data for the pre-contrast, arterial, portal venous, transitional, and hepatobiliary phases.

[†]Data are shown as phase direction acceleration factor × partition direction acceleration factor. MRI, magnetic resonance imaging; SSAP, second-shot arterial phase.

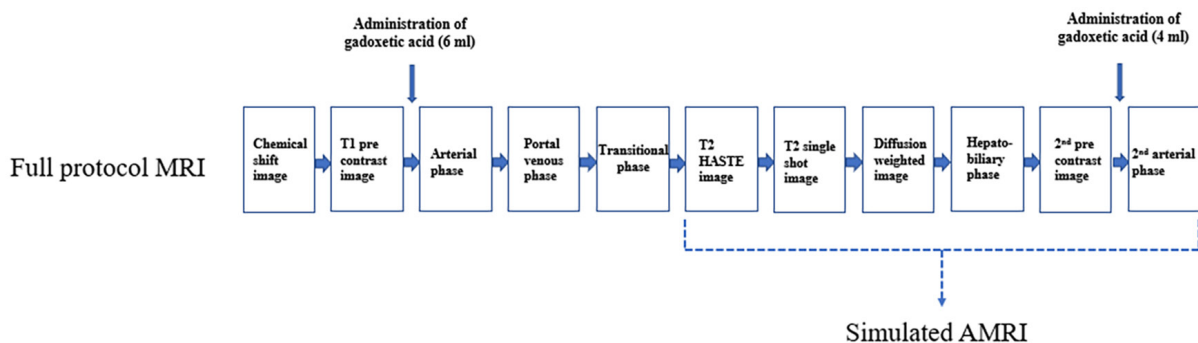


Figure 2. Liver magnetic resonance imaging with modified injection protocol. MRI, magnetic resonance imaging; AMRI, abbreviated liver magnetic resonance imaging.

ing a modified version of the LI-RADS treatment response algorithm. Ancillary features, such as diffusion restriction and T2-weighted mild to moderate hyperintensity, were also optionally used.

Disagreements during the review sessions regarding the motion artifact score and categorizations using LR-TR and abblR-TR in the targeted lesions were resolved by consensus.

Scan time

For the patients included in the study, one board-certified radiologist compared the scan time between the FP-MRI and simulated AMRI.

Statistical analysis

The scan time between the two protocols (FP-MRI and simulated AMRI) was compared using the Student's t-test. Per-lesion sensitivity and specificity were compared between the two imaging sessions using McNemar's test. The Wilcoxon rank-sum test was used to compare the motion scores between routine AP and each phase of the SSAP in the FP-MRI. We evaluated the inter-observer agreement for the viability evaluation of treated lesions and motion artifact scores using Cohen's kappa. Agreement was defined as poor ($\kappa=0-0.20$), fair ($0.21-0.40$), moderate ($0.41-0.60$), good ($0.61-0.80$), or excellent ($0.81-1.00$). Statistical significance was set at $P < 0.05$. All statistical analyses were conducted using the SPSS software for Windows (v.27.0; IBM Corp., Armonk, NY, USA).

Result

Patient demographics

A total of 132 patients underwent gadoxetic acid-enhanced MRI with modified injection after LRT for HCC. After exclusion, 95 patients with treated observations and their reference standards (95 observations of the largest target for each patient) were included in the study (Figure 1). The causes of chronic liver disease in the patients were chronic hepatitis B ($n = 59$), chronic hepatitis C ($n = 22$), alcohol ($n = 13$), and others ($n = 1$). Of the 95 patients, 42 (44.2%) had viable lesions and 53 (55.8%) had non-viable lesions. Tumor viability was assessed using histopathology and DSA. Only three viable lesions and one non-viable lesion were confirmed surgically. Other lesions were confirmed using DSA (Table 2).

Scan time

The scan time of the simulated AMRI was significantly shorter compared with the FP-MRI (7.6 ± 0.49 and 23.6 ± 0.50 minutes, respectively; $P < 0.001$).

Diagnostic performance for evaluating viability of treated HCC in the abbreviated liver and full-protocol magnetic resonance imaging

Using the FP-MRI, 36, 5, and 1 lesions were assigned to the LR-TR viable, LR-TR equivocal, and LR-TR non-viable categories, respectively, among 42 viable lesions. Using the AMRI with SSAP, 34, 6, and 2 lesions were assigned to the abblR-TR viable, abblR-TR equivocal, and abblR-TR non-viable categories, respectively, among 42 viable lesions. For evaluating the viability of treated HCC, no significant differences were observed in the sensitivity and specificity between the FP-MRI and AMRI with SSAP [sensitivity, 85.7% (36/42) vs. 80.1% (34/42), respectively, $P = 0.500$; speci-

ficity, 96.2% (51/53) vs. 96.2% (51/53), respectively, $P = 1.000$] (Table 3, Figures 3, and 4).

Comparison of the respiratory motion artifacts between the original arterial phase and the second-shot arterial phase

The mean motion score of the original AP was significantly higher compared with the three SSAPs (1.25 vs. 1.04, 1.02, and 1.01; all $P < 0.001$) (Table 4). TSM was not observed in the original AP and SSAP.

Inter-observer agreement

Inter-observer agreement was good for the viability of the target lesion using the LR-TR algorithm in the FP-MRI and the abblR-TR category in the AMRI with SSAP ($k = 0.79$ and $k = 0.79$, respectively). The inter-observer agreements were good for the motion scores on the original AP and the three SSAPs ($k = 0.76$ and $k = 0.65$, 0.66, and 0.66, respectively).

Table 2. Patient demographics

Characteristics	Patients
Age	68.7 years old
Male: female	70: 25
Etiology	
Chronic hepatitis B	59
Chronic hepatitis C	22
Alcohol	13
Others	1
Child-Pugh classification	
Previous locoregional treatment	
RFA	22
TACE	73
Reference standards for tumor viability	
Viable	42
Pathologically confirmed	3
Confirmed with DSA	39
Non-viable	53
Pathologically confirmed	1
Clinically confirmed	52
Previous gadoxetic acid-enhanced MRI	88

RFA, radiofrequency ablation; TACE, transcatheter arterial chemoembolization; MRI, magnetic resonance imaging; DSA, digital subtraction angiography.

Table 3. Diagnostic performance for the full-protocol MRI and AMRI with SSAP

	Full protocol MRI	AMRI with SSAP	P value
Sensitivity	36/42	34/42	0.500
Specificity	51/53	51/53	1.000

MRI, magnetic resonance imaging; AMRI, abbreviated liver magnetic resonance imaging; SSAP, second-shot arterial phase.

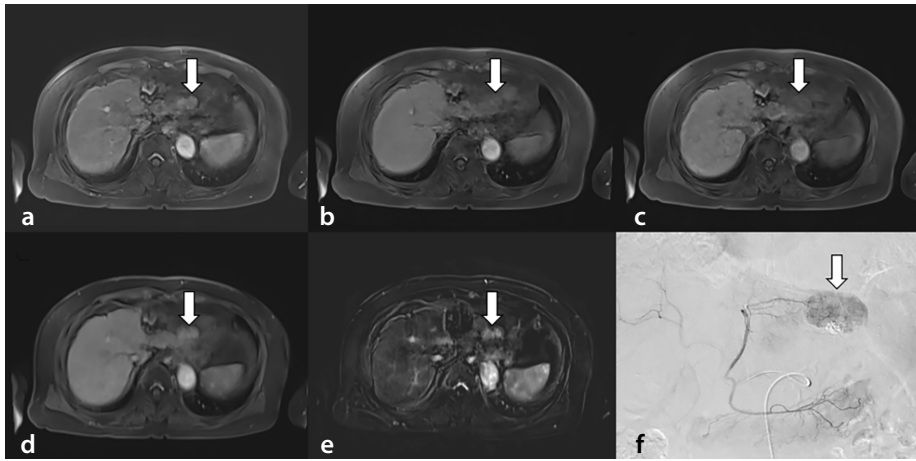


Figure 3. Hepatocellular carcinoma treated with transcatheter arterial chemoembolization (TACE) in a 60-year-old male. On gadolinic acid-enhanced liver magnetic resonance imaging, a TACE-treated lesion (arrow) in segment II shows mass-like arterial enhancement and washout in the original arterial phase image (a) and portal venous phase (b), respectively. In the hepatobiliary phase, it shows hypointensity (arrow) (c). The second-shot arterial phase images, with or without subtraction, demonstrate mass-like arterial enhancement on the treated lesion (d and e). This treated lesion is assigned as Liver Imaging Reporting and Data System treatment response (LR-TR)-viable. When applying the abbreviated LR-TR (abbLR-TR) category, it is assigned as abbLR-TR-viable. The digital subtraction angiography examination demonstrates the presence of the tumor stain (arrow) in the subsequent TACE session (f).

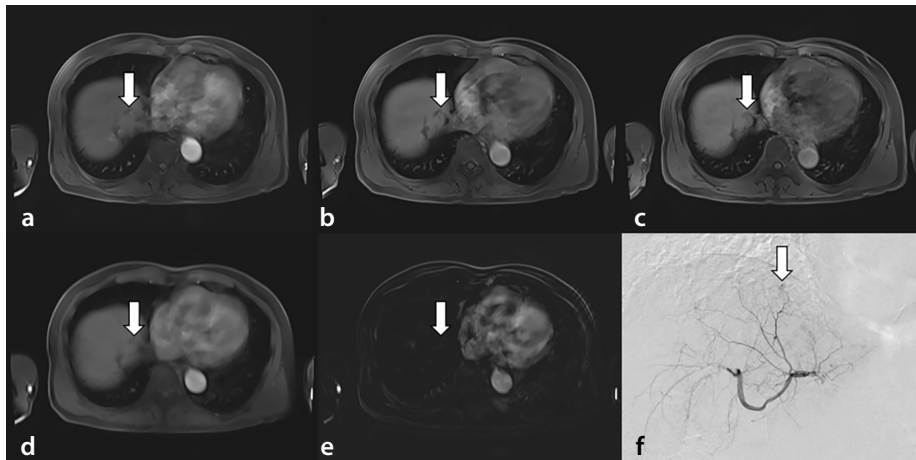


Figure 4. Hepatocellular carcinoma treated with transcatheter arterial chemoembolization (TACE) in a 63-year-old male. On gadolinic acid-enhanced liver magnetic resonance imaging, a TACE-treated lesion (arrow) in the liver dome shows mass-like arterial enhancement and no washout in the original arterial phase image (a) and portal venous phase (b), respectively. In the hepatobiliary phase, it shows hypointensity (arrow) (c). The second-shot arterial phase images, with or without subtraction, demonstrate no mass-like arterial enhancement on the treated lesion (d and e). This treated lesion is assigned as Liver Imaging Reporting and Data System treatment response (LR-TR)-viable. When applying the abbreviated LR-TR (abbLR-TR) category, it is assigned as abbLR-TR non-viable. The digital subtraction angiography examination demonstrates the presence of the tumor stain (arrow) in the subsequent TACE session (f).

Table 4. Mean motion scores		
	Mean motion score	P value (vs. original AP)
Original AP	1.25	
SSAP1	1.04	<0.001
SSAP2	1.02	<0.001
SSAP3	1.01	<0.001

AP, arterial phase; SSAP, second-shot arterial phase.

Discussion

In this study, the scan time of the simulated AMRI was significantly shorter compared with the FP-MRI. Contrastingly, the abbLR-TR category in the AMRI with SSAP showed diagnostic performance comparable to that of the LR-TR algorithm in the FP-MRI. In addition, the mean motion score of the original AP was significantly higher than that of SSAP.

In previous studies on SSAP, the image acquisition times for AMRI were significantly shorter; they also demonstrated no significant difference between the FP-MRI and AMRI with SSAP in the diagnosis of HCC or hepatic metastasis,^{18,19} which are consistent with our results. However, our study focused on the viability of HCC after LRT.

In the current study, the reference standards for tumor viability included only a few pathologically confirmed results [viable, 7.1% (3/42); non-viable, 1.9% (1/53)]. In a previous meta-analysis for the LR-TR algorithm, the pooled specificity and sensitivity of the LR-TR viable category were 96% [95% confidence interval (CI): 91%–99%] and 63% (95% CI: 39%–81%), respectively.²⁰ The same study also conducted a meta-regression study for the reference standard. The researchers reported that studies using reference standard to imaging findings (imaging follow-up or imaging/pathologic results) demonstrated significantly higher sensitivity compared to those using pathology alone (81% vs. 48%, respectively). However, LR-TR v2024 was not adopted in the studies included in the meta-analysis. Recently, Zhou et al.²¹ reported that LI-RADS non-radiation TRA v.2024 improved the sensitivity (85.5% and 87.2%) of assessing the viability of treated HCC, using ancillary features with reference to the only pathologic results. The sensitivity of our study for treated lesions with FP-MRI and AMRI with SSAP was 85.7% and 80.9%, respectively. In addition, the specificities were 96.2% for both protocols. Accordingly, our results showed a diagnostic performance comparable to those of previous studies. However, further studies evaluating the diagnostic performance of LR-TR A v.2024 are required.

Hepatobiliary-specific MR contrast agents (e.g., gadolinic acid, gadobenate dimeglumine, mangafodipir trisodium) have previously been used in the diagnosis of HCC. These contrast agents, taken up by hepatocytes, can provide the T1 shortening effect of normal liver parenchyma, resulting in high signal intensity on HBP. For gadolinic acid, 50% of the injected contrast media is

transported to hepatocytes. Gadoteric acid acts as an extracellular contrast agent in the arterial and portal venous phases. In addition, an HBP image can be obtained with a relatively short delay of 10–20 minutes after injection.²² Therefore, gadoteric acid is useful for the detection of HCC.^{23,24} In evaluating the viability of treated HCC using gadoteric acid-enhanced liver MRI, the HBP image can aid in the detection of a lesion treated with LRT. However, according to LR-TR v.2024, HBP hypointensity is not accepted as an ancillary feature for assessing the viability of treated HCC. Accordingly, it was not applied in either the FP-MRI or AMRI in this study. Although the presence of HBP hypointensity is not a major or ancillary feature in the LR-TR v.2024, the inclusion of an HBP image may be necessary for the AMRI protocol for assessing the viability of treated HCC after LRT. This is because the detection of newly developed HCC is also clinically important for patients with a history of LRT. For treatment-naïve lesions, HBP hypointensity was reported as a useful feature for the detection of HCC. Kim et al.²³ reported that the extension of washout to the transitional phase or HBP allowed for higher sensitivity without a reduction in specificity, rather than restricting it to the PVP after excluding typical hemangiomas and nodules with a targetoid appearance. In another study by Joo and colleagues, the diagnostic criteria extending washout to the HBP demonstrated higher sensitivity than those limiting washout to the PVP, with little loss of specificity.²⁴

Recently, LR-TR v.2024 adopted a single major feature, “mass-like enhancement (any degree, any phase)” for assessing the viability of treated HCC on CT or MRI.⁵ After LRT of the hypervascular HCC, the representative imaging finding suggesting viable HCC is “mass-like enhancement (any degree, any phase)”. Zhou et al.²¹ reported that LI-RADS non-radiation TRA v.2024 without ancillary features, using a single major feature, “mass-like enhancement (any degree, any phase)” for assessing the viability of treated HCC, demonstrated higher sensitivity than LI-RADS TRA v.2017 (80.3% and 81.1% vs. 79.1% and 79.9%, respectively). This result supports the diagnostic value of “mass-like enhancement (any degree, any phase)” as representative imaging findings, suggesting viable HCC. Zhou et al.²¹ also reported that LI-RADS non-radiation TRA v.2024 with ancillary features provided significantly higher sensitivity than LI-RADS TRA v.2017 (85.5% and 87.2% vs. 79.9% and 79.1%; all $P < 0.001$). This re-

sult emphasized the importance of the ancillary features, such as diffusion restriction and mild-to-moderate T2 hyperintensity, in evaluating the viability of treated HCC after radiation-free LRT. In addition, this result supports the inclusion of diffusion-weighted imaging and T2-weighted imaging in the AMRI protocol for assessing the viability of treated HCC after LRT.

The mean motion score of the original AP was significantly higher than that of the three SSAPs. These results are consistent with those of Park et al.¹⁷ However, TSM was not observed in our group. A previous study including a large number of patients demonstrated that the presence of hepatitis B and previous experience with gadoteric acid-enhanced MRI were negative risk factors for TSM.²⁵ Our study also included a large portion of patients with previous experience with gadoteric acid-enhanced MRI (88/95) and chronic hepatitis B (59/95). These factors are believed to be the reasons for the lack of TSM. In addition to the relative motion insensitivity of SSAP, the multiple APs (three-phase, in our study) of SSAP may also be one of the reasons for the non-inferior sensitivity to FP-MRI in our study. In a previous study conducted by Hong et al.¹⁵, multiple APs had a lower incidence of TSM than single AP and significantly improved sensitivity for diagnosing HCC (≤ 3 cm), without a significant decrease in specificity.

This study has some limitations. First, it was a retrospective study that included a relatively small number of patients; thus, there may have been selection bias. However, the data collection was performed consecutively. A prospective study is required to evaluate the diagnostic performance of AMRI using SSAP. Second, reference standards for tumor viability included few pathologically confirmed results [viable, 7.1% (3/42); non-viable, 1.9% (1/53)], and our study included patients treated with only non-radiation LRT. However, the diagnostic performance of the abblR-TR category for AMRI with SSAP was not significantly different from that reported in previous studies.^{20,21}

In conclusion, the abblR-TR category in the AMRI with SSAP showed non-inferior diagnostic performance compared to FP-MRI in evaluating the viability of the treated HCC after non-radiation LRT. Therefore, this abbreviated protocol may serve as a faster and more convenient alternative for post-treatment surveillance following non-radiation LRT.

Footnotes

Conflict of interest disclosure

The authors declared no conflicts of interest.

References

1. Allard MA, Sebahg M, Ruiz A, et al. Does pathological response after transarterial chemoembolization for hepatocellular carcinoma in cirrhotic patients with cirrhosis predict outcome after liver resection or transplantation? *J Hepatol.* 2015;63(1):83-92. [\[CrossRef\]](#)
2. Ho MH, Yu CY, Chung KP, et al. Locoregional therapy-induced tumor necrosis as a predictor of recurrence after liver transplant in patients with hepatocellular carcinoma. *Ann Surg Oncol.* 2011;18(13):3632-3639. [\[CrossRef\]](#)
3. Chernyak V, Fowler KJ, Kamaya A, et al. Liver Imaging Reporting and Data System (LI-RADS) version 2018: imaging of hepatocellular carcinoma in at-risk patients. *Radiology.* 2018;289(3):816-830. [\[CrossRef\]](#)
4. Kielar A, Fowler KJ, Lewis S, et al. Locoregional therapies for hepatocellular carcinoma and the new LI-RADS treatment response algorithm. *Abdom Radiol (NY).* 2018;43(1):218-230. [\[CrossRef\]](#)
5. American College of Radiology website. LI-RADS Ct/Mri Nonradiation Tra V2024 Core 2024 [cited 2024 Apr 18]. [\[CrossRef\]](#)
6. Sun HY, Lee JM, Shin CI, et al. Gadoteric acid-enhanced magnetic resonance imaging for differentiating small hepatocellular carcinomas (< or =2 cm in diameter) from arterial enhancing pseudolesions: special emphasis on hepatobiliary phase imaging. *Invest Radiol.* 2010;45(2):96-103. [\[CrossRef\]](#)
7. Kim YK, Lee MW, Lee WJ, et al. Diagnostic accuracy and sensitivity of diffusion-weighted and of gadoteric acid-enhanced 3-T MR imaging alone or in combination in the detection of small liver metastasis (≤ 1.5 cm in diameter). *Invest Radiol.* 2012;47(3):159-166. [\[CrossRef\]](#)
8. Park YS, Lee CH, Kim JW, Shin S, Park CM. Differentiation of hepatocellular carcinoma from its various mimickers in liver magnetic resonance imaging: what are the tips when using hepatocyte-specific agents? *World J Gastroenterol.* 2016;22(1):284-299. [\[CrossRef\]](#)
9. Davenport MS, Viglianti BL, Al-Hawary MM, et al. Comparison of acute transient dyspnea after intravenous administration of gadoterate disodium and gadobenate dimeglumine: effect on arterial phase image quality. *Radiology.* 2013;266(2):452-461. [\[CrossRef\]](#)
10. Hong SB, Lee NK, Kim S, et al. Modified CAIPIRINHA-VIBE without view-sharing on

- gadoteric acid-enhanced multi-arterial phase MR imaging for diagnosing hepatocellular carcinoma: comparison with the CAIPIRINHA-Dixon-TWIST-VIBE. *Eur Radiol.* 2019;29(7):3574-3583. [\[CrossRef\]](#)
11. Pietryga JA, Burke LM, Marin D, Jaffe TA, Bashir MR. Respiratory motion artifact affecting hepatic arterial phase imaging with gadopentate disodium: examination recovery with a multiple arterial phase acquisition. *Radiology.* 2014;271(2):426-434. [\[CrossRef\]](#)
 12. Park YS, Lee CH, Kim IS, et al. Usefulness of controlled aliasing in parallel imaging results in higher acceleration in gadoteric acid-enhanced liver magnetic resonance imaging to clarify the hepatic arterial phase. *Invest Radiol.* 2014;49(3):183-188. [\[CrossRef\]](#)
 13. Yoo JL, Lee CH, Park YS, et al. The short breath-hold technique, controlled aliasing in parallel imaging results in higher acceleration, can be the first step to overcoming a degraded hepatic arterial phase in liver magnetic resonance imaging: a prospective randomized control study. *Invest Radiol.* 2016;51(7):440-446. [\[CrossRef\]](#)
 14. Yoon JH, Lee JM, Yu MH, et al. Evaluation of transient motion during gadoteric acid-enhanced multiphasic liver magnetic resonance imaging using free-breathing golden-angle radial sparse parallel magnetic resonance imaging. *Invest Radiol.* 2018;53(1):52-61. [\[CrossRef\]](#)
 15. Hong SB, Hong S, Choi SH, et al. Multiple arterial-phase mri with gadoteric acid improves diagnosis of hepatocellular carcinoma ≤ 3.0 cm. *Liver Int.* 2023;43(2):462-470. [\[CrossRef\]](#)
 16. Polanec SH, Bickel H, Baltzer PAT, et al. Respiratory motion artifacts during arterial phase imaging with gadoteric acid: can the injection protocol minimize this drawback? *J Magn Reson Imaging.* 2017;46(4):1107-1114. [\[CrossRef\]](#)
 17. Park YS, Lee J, Kim JW, Park CM, Lee CH. Second shot arterial phase to overcome degraded hepatic arterial phase in liver MR imaging. *Eur Radiol.* 2019;29(6):2821-2829. [\[CrossRef\]](#)
 18. Kim JW, Lee CH, Park YS, Lee J, Kim KA. Abbreviated gadoteric acid-enhanced MRI with second-shot arterial phase imaging for liver metastasis evaluation. *Radiol Imaging Cancer.* 2019;1(1):e190006. [\[CrossRef\]](#)
 19. Kim JW, Lee CH, Kim KA, Lee J, Park YS. Abbreviated MRI with second shot arterial phase for HCC evaluation: modified version of LI-RADS and recall reduction strategy. *Eur Radiol.* 2023;33(6):4401-4411. [\[CrossRef\]](#)
 20. Youn SY, Kim DH, Choi SH, et al. Diagnostic performance of Liver Imaging Reporting and Data System treatment response algorithm: a systematic review and meta-analysis. *Eur Radiol.* 2021;31(7):4785-4793. [\[CrossRef\]](#)
 21. Zhou S, Zhou G, Shen Y, et al. LI-RADS nonradiation treatment response algorithm version 2024: diagnostic performance and impact of ancillary features. *AJR Am J Roentgenol.* 2025;224(2):e2432035. [\[CrossRef\]](#)
 22. Seale MK, Catalano OA, Saini S, Hahn PF, Sahani DV. Hepatobiliary-specific MR contrast agents: role in imaging the liver and biliary tree. *Radiographics.* 2009;29(6):1725-1748. [\[CrossRef\]](#)
 23. Kim DH, Choi SH, Kim SY, Kim MJ, Lee SS, Byun JH. Gadoteric acid-enhanced MRI of hepatocellular carcinoma: value of washout in transitional and hepatobiliary phases. *Radiology.* 2019;291(3):651-657. [\[CrossRef\]](#)
 24. Joo I, Lee JM, Lee DH, Jeon JH, Han JK. Retrospective validation of a new diagnostic criterion for hepatocellular carcinoma on gadoteric acid-enhanced MRI: can hypointensity on the hepatobiliary phase be used as an alternative to washout with the aid of ancillary features? *Eur Radiol.* 2019;29(4):1724-1732. [\[CrossRef\]](#)
 25. Jang EB, Kim DW, Choi SH, et al. Transient severe motion artifacts on gadoteric acid-enhanced mri: risk factor analysis in 2230 patients. *Eur Radiol.* 2022;32(12):8629-8638. [\[CrossRef\]](#)